ELSEVIER

Polymer 40 (1998) 171–181

polymer

Formation and structure of the epoxy–silica hybrids

Libor Matějka*, Karel Dušek, Josef Pleštil, Jaroslav Kříž, František Lednický

Institute of Macromolecular Chemistry, Academy of Sciences of the Czech Republic, 162 06 Prague 6, Czech Republic

Received 13 February 1997; revised 9 January 1998; accepted 10 March 1998

Abstract

The organic–inorganic hybrid interpenetrating network (IPN) composed of an epoxide–amine network and silica was prepared and studied. Formation of the inorganic phase from tetraethoxysilane (TEOS) by sol–gel process was characterized by ^{29}Si n.m.r. spectroscopy, gas chromatography, small-angle X-ray scattering and electron microscopy. Kinetics of the silica structure build-up in the organic matrix, its final structure and morphology depend on the method of IPN hybrid preparation. The large compact silica aggregates, 100–300 nm in diameter, are formed during the one-stage polymerization. The two-stage process with the acid prehydrolysis of TEOS leads to an acceleration of gelation and formation of more open and smaller silica structures: 50–100 nm in diameter. The most homogeneous hybrid morphology with the smallest silica domains of size 10–20 nm, appears in the sequential IPN. The development of the silica structure is restricted by a rigid reaction medium of the preformed epoxide network.

Keywords: Organic–inorganic hybrids; Interpenetrating networks; Sol–gel process

1. Introduction

In recent years an intense research has been devoted to the study of organic–inorganic hybrid systems [1–9]. The low-temperature sol–gel process starting from organometallic precursors such as silicates, titanates and aluminates, has been a convenient technique for synthesis of the inorganic part of these hybrids. Tetraethoxysilane (TEOS) is the most common precursor yielding a glassy silica network by hydrolysis and condensation. The sol–gel process is acid- and base-catalysed and the type of catalysis, water amount, solvent and temperature affect the resulting structure of the silica [1,8]. The kinetics of the process including the simultaneous hydrolysis and condensation was generally studied by Assink and Kay [10].

The structure of the silica often shows a selfsimilar fractal behaviour [11] and may be characterized using the concept of fractal geometry which is often applied to describe the structure of randomly formed objects. The important characteristics of the fractal are the mass fractal dimension D_m providing information about the distribution of mass m in a volume: $m \sim r^{Dm}$, where r is the radius of the fractal object and the relation $1 < D_m < 3$ holds for the mass fractal. The mass fractal dimension is a measure of the compactness or shape of the object. The structure formed during the sol–gel process and the corresponding fractal dimension are determined by the mechanism of polymerization and/or aggregation and kinetic growth models are used to describe the structure development. Two types of growth processes are taken into account in the case of silicate systems; reaction-limited cluster–cluster (RLCCA) and monomer–cluster (RLMCA) aggregation [12]. Computer simulation predicts the value of fractal dimension $D_m = 2.1$ for RLCCA and $D_m = 3.0$ for RLMCA. Experimental SAXS studies have shown [1] that mass fractal polymers with $D_m = 2.1$ are formed during acid catalysis of the sol–gel process which is consistent with the cluster–cluster reaction. In the case of base catalysis the monomer–cluster aggregation is operative and more compact mass or surface fractals corresponding to colloidal particles were determined.

The 'ceramers' or 'ormosils', materials combining *cera*mic and poly*mer*ic behaviour [2,3] or *or*ganically *mo*dified *sil*icates [4], are synthesized from organic polymers and inorganic components. In situ polymerization of TEOS in an organic polymer medium results in formation of an inhomogeneous system. Wilkes' morphological model [2] describes an organic–inorganic hybrid as a polymer-rich matrix with dispersed silica-rich domains and mixed phase of partly condensed siloxane clusters and an organic polymer. Finely dispersed silica phase can act as a polymer filler and inhomogeneities of various size may be formed. They are usually of nanometer size and the arising transparent

* Corresponding author.

0032-3861/98/$ - see front matter
PII: S0032-3861(98)00214-6

'nanocomposites' offer a variety of advantageous properties in various applications. They can be employed as optical materials [13] with high refractive indices, coloured glasses [14], hard coating on soft surfaces [15], porous materials for chromatographic and catalyst [16] supports, aerogels [17] with extremely low density, materials with increased thermal stability and inflammability for encapsulation of biosensors [18], etc. The combination of hardness of an inorganic glass and toughness of an organic polymer makes such a system interesting also from the perspective of mechanical behaviour. Toughening of a brittle inorganic glass or an increase of the hardness for scratch-resistant polymeric coatings may be examples of application of the sol–gel hybrid materials and chemistries.

We have studied an interpenetrating network (IPN) of the organic–inorganic hybrid system composed of an organic polymer network and an inorganic silica structure formed by a sol–gel process from TEOS. The organic system was represented by a stoichiometric epoxide–amine rubbery network prepared from diglycidyl ether of Bisphenol A (DGEBA) and poly(oxypropylene)diamine, Jeffamine® D 2000. The *in-situ* built-in inorganic phase results in reinforcement of the rubbery network. During polymerization grafting between the epoxide network and silica–siloxane structures also takes place by condensation of silanol groups with the C–OH group formed at the epoxide–amine reaction [19]. The goal of this paper is to investigate the formation of the hybrid DGEBA–D2000–TEOS and to determine factors governing its morphology and structure that were characterized by scanning electron microscopy (SEM) and by small-angle X-ray scattering (SAXS). The effect of type of the catalyst for the sol–gel process, in particular of the amine hardener D2000 acting as a nucleophilic polymeric catalyst and the influence of the presence of the epoxide network on the formation of the silica phase were studied. The results are compared with those of Bauer *et al.* [19], who also investigated the epoxy–silica IPN.

2. Experimental

2.1. Organic system components

The epoxide network was prepared by curing diglycidyl ether of Bisphenol A (DGEBA) with poly(oxypropylene)-diamine, Jeffamine® D2000 (M = 1970). The equivalent weights per functional group, the epoxide group in DGEBA and NH group in Jeffamine® D2000, were, respectively, E_E = 171 g/mol and E_{NH} = 492 g/mol.

2.2. Inorganic system components

Tetraethoxysilane (TEOS) was used as received (Fluka) (99.3%, gas chromatography analysis). Catalysts: *p*-toluenesulfonic acid monohydrate (TSA) was purified by multiple recrystallization from methanol (melting point 103°C). Benzyldimethylamine (BDMA) and dibutyltin dilaurate (DBTDL) were used as received.

2.3. Sol–gel process

Hydrolysis and polymerization of TEOS was performed in isopropyl alcohol (IP) solutions using variable concentrations of a catalyst. Ethyl alcohol (EtOH) solutions were applied to n.m.r. measurements. The volume ratio TEOS:IP = 45:55 and molar ratio TEOS:H_2O = 1:3 were used in most experiments.

2.4. Synthesis of the hybrid system

The hybrids were composed of a stoichiometric mixture of the organic components, DGEBA and D2000 (the ratio of functionalities C_{NH}/C_{epoxy} = 1) and the inorganic phase components—TEOS and H_2O. TSA (2 mol% relative to the content of TEOS) was used as a catalyst. Three ways of synthesis procedures were employed.

2.4.1. One-step procedure

All reaction components were mixed and reacted. The system was kept 2 h at room temperature, heated to 90°C for 2 days and cured and dried in vacuum at 130°C for 2 days. The hybrid composition corresponded to ratios of functionalities DGEBA:D2000:TEOS = 1:1:9.5.

2.4.2. Two-step procedure with prehydrolysed TEOS

(1) TEOS was prehydrolysed in the presence of TSA at room temperature for 1 h. (2) The hydrolysed TEOS was mixed with the organic phase components DGEBA and D2000. The hybrid composition and the subsequent curing procedure were the same as in the case of the one-stage process.

2.4.3. Two-step procedure with preformed epoxide network

(1) The stoichiometric epoxide–amine network was prepared first by curing DGEBA with D2000 at an equivalent ratio of functional groups for 16 h at 90°C and 2 h at 130°C. (2) The network was swollen in the mixture TEOS–H_2O–IP at room temperature for 24 h up to equilibrium. The content of silica in the hybrid depended on the composition of the swelling medium TEOS–IP ranging from 5:95 to 40:60 by volume. The swollen network was placed in a polypropylene sack and heated at 90°C for 5 days to polymerize TEOS and to develop the inorganic silica phase within the epoxide network. Final curing and drying was performed in vacuum at 130°C for 2 days.

2.5. Analysis

Gas chromatography analysis was performed using Perkin Elmer 8310 apparatus. The time of gelation was evaluated visually as a time when the flow of the reaction mixture stopped. The silica content in hybrid networks was

determined by treatment of the sample with sulphuric acid and its combustion to constant weight.

2.6. ^{29}Si n.m.r. spectroscopy

^{29}Si and ^{1}H n.m.r. spectra were measured in solution in 5-mm tubes at 39.7 (^{29}Si) and 200.0 (^{1}H) MHz with a Varian Unity 200 n.m.r. spectrometer, mostly at 21°C. For ^{1}H n.m.r., repetition time 12 s with $\pi/6$ flipping pulse was found to be sufficient for quantitative results. ^{29}Si spectra were measured by the ^{1}H–^{29}Si polarization transfer using the DEPT sequence. The proton relaxation delay of 9 s and the polarization transfer period 0.142 s (corresponding to $J_{H\text{-}Si} = 3.5$ Hz) were found to be optimum for both sensitivity and quantitative reliability of the signal intensities. Usually, 128 scans were accumulated and exponential weighting with the line-broadening factor lb = 1.0 was used before FT.

Different types of structural bound Si atoms involved in hydrolysed and condensed species were indicated as usual, Q_i^j, where i and j represent number of siloxane bonds -$OSiR_3$ and number of -OH groups attached to the Si atom, respectively. Assignment of the corresponding bands of ^{29}Si n.m.r. spectrum in the region from -70 up to -100 ppm was taken from the literature [20,21] for systems dissolved in EtOH. The chemical shifts were different using IP as a diluent. The Si atoms with no connection to an unreacted -OCH_2CH_3 group, i.e., fully hydrolysed species Q_0^4, Q_1^3, Q_2^2 and Q_1^3, give no signal in DEPT measurements and their content was evaluated by combination of ^{29}Si n.m.r. and ^{1}H n.m.r. spectra as follows.

^{1}H n.m.r. measurements were employed to follow the kinetics by determination of the concentration of EtOH formed during hydrolysis and alcohol-producing condensation by using the relative fraction of CH_2 group signals corresponding to HO-$\underline{CH_2}$-CH_3 and to Si derivatives ≡Si-O-$\underline{CH_2}$-CH_3, respectively. Hydrolysis of the ≡Si-OC_2H_5 group results in releasing 1 molecule of EtOH and one more molecule of EtOH forms in the condensation. In total, 2 molecules of EtOH are released to form the siloxane bond ≡Si-O-Si≡ in the condensed species. The relative content of the EtOH formed with respect to the Si derivatives can be calculated from fraction concentrations of the hydrolysed and condensed species; [EtOH] = C + C_1, where

$$C = \frac{Q_0^1}{4} + \frac{Q_0^2}{2} + \frac{3Q_0^3}{4} + \frac{Q_1^0}{3} + \frac{Q_1^1}{2} + \frac{3Q_1^2}{4} + \frac{Q_2^0}{2} + \frac{3Q_2^1}{4} + \frac{3Q_3^0}{4}$$

and $C_1 = Q_0^4 + Q_1^3 + Q_2^2 + Q_3^1$ are overall relative concentrations of the hydrolysed species determined by ^{29}Si n.m.r. and species invisible in ^{29}Si n.m.r., respectively.

The content of the invisible species C_1 was determined as the difference between the EtOH content evaluated by ^{1}H n.m.r. and sum C determined by ^{29}Si n.m.r. Concentrations of particular species were estimated from the best computer fit of the experimental data.

2.7. Small-angle X-ray scattering (SAXS)

SAXS experiments were done by using a Kratky camera (A. Paar KG, Graz) with a slit collimation. Scattering curves were converted to the absolute scale by means of Lupolen standards, using the formula [22]

$$d\sum \frac{\tilde{\Sigma}}{d\Omega}(q) = \frac{a}{I_L K_L T_d}\tilde{I}(q)$$

where $\tilde{I}$(q) is the measured scattering intensity, a is the sample-detector distance, T is the sample transmission, d is the sample thickness, K_L is a calibration constant, I_L is the intensity of radiation scattered by the standard at $q = (2\pi/150$ Å), $q = (4\pi/\lambda)\sin\theta$ is the magnitude of the scattering vector, λ is the wavelength of radiation and 2θ is the scattering angle. The differential scattering cross-section $d\Sigma/d\Omega\,(q)$ in cm^{-1} referred to as intensity I can be then obtained by means of the desmearing program ITR [23]. As the collimation did not provide unambiguous results in all cases, we present here the experimental (smeared) scattering curves.

The shape of a scattering curve gives an information about size and structure of domains in the system. A linear dependence of the double logarithmic plot of the scattered intensity I *versus* the scattering vector q over a broad range of q characterizes fractal objects. The mass fractal dimension D_m of the silica phase formed during the sol–gel process can be determined from the region of the power-law decay of the scattered intensity: $I \sim q^{-x}$ as the slope x of the logarithmic plot; $D_m = x$ for $1 < x < 3$. The exponents $3 < x < 4$ indicate surface fractals. For an infinite slit length the experimental slope $\tilde{x}$ determined from a slit smeared intensity ($\tilde{I} \sim q^{-\tilde{x}}$) is related to the exponent x corresponding to the point collimation, $x = \tilde{x} + 1$. The size of heterogeneities was estimated using the expression $d = 2\pi/q_{min}$ [24] where q_{min} is a minimum q corresponding to the linear part of the scattering curve.

2.8. Electron microscopy (SEM)

Fracture surfaces of the samples were examined to reveal their supermolecular structure: samples (with a soft matrix) were provided with a razor-blade notch and fractured in tension (soft matrix fracture surface). The samples were sputter-coated with a platinum layer (thickness 3 nm), observed and micrographed, using a JEOL JSM 6400 scanning electron microscope.

3. Results and discussion

The course of the sol–gel process, of the inorganic phase gelation, the morphology and structure of the hybrid interpenetrating network DGEBA–D2000–TEOS were investigated. In addition, the model TEOS system polymerized under the same conditions was studied for comparison. The acid TSA, pH neutral DBTDL and a Lewis base,

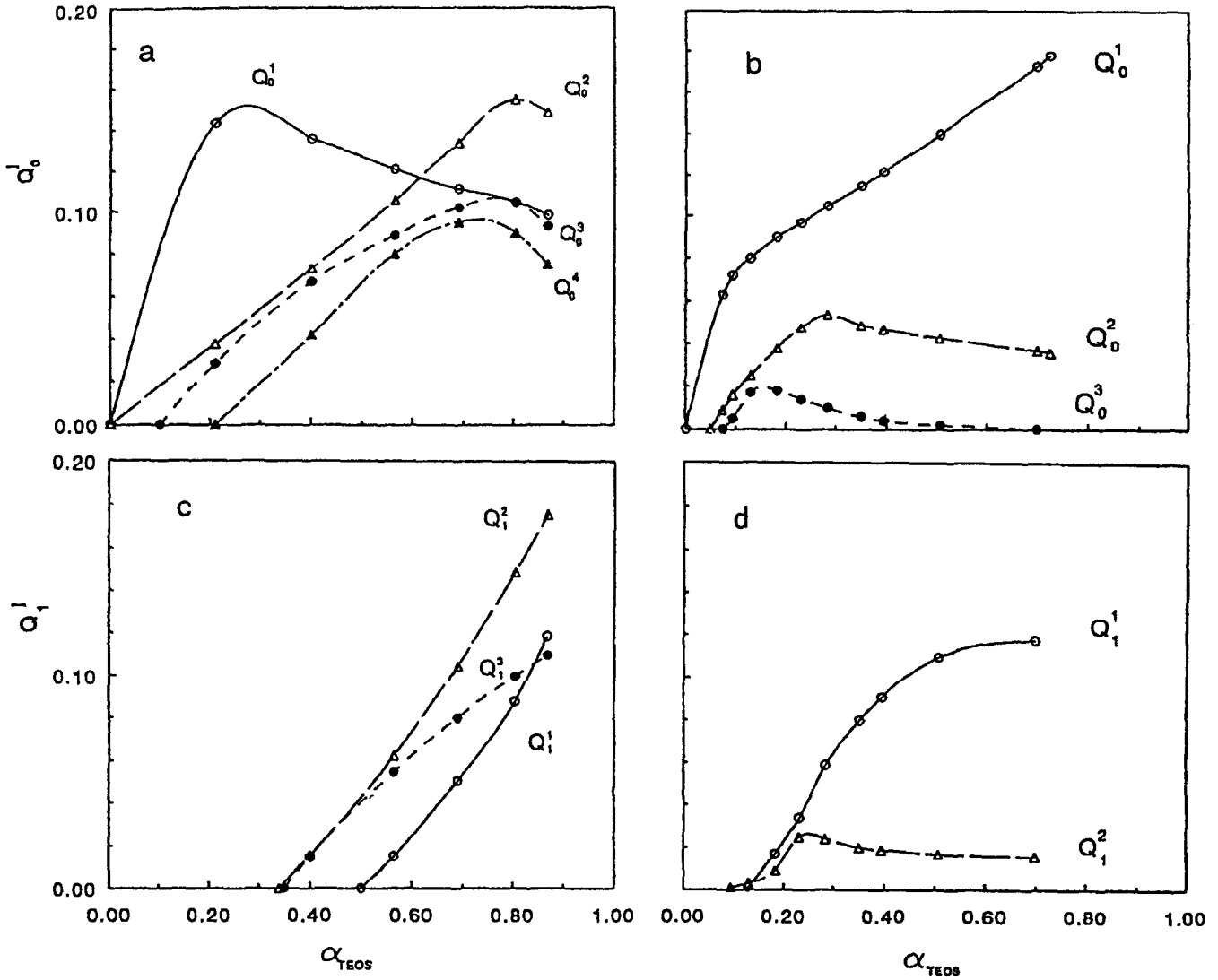

Fig. 1. Development of fractions of the hydrolysed and condensed species Q_0^j and Q_1^j as a function of TEOS conversion, α_{TEOS}, in the polymerization of TEOS by the sol–gel process as determined by n.m.r. (a), (c) catalysis by 2 mol% TSA/TEOS (relative to TEOS). (b), (d) catalysis by 2 mol% BDMA/TEOS

BDMA, were employed to catalyse the sol–gel process. Moreover, the catalytic effect of D2000 was studied. The rate of conversion and gelation of TEOS as well as the resulting morphology formed under different catalyses are given in Table 1.

3.1. Hydrolysis and condensation of TEOS

^{29}Si and ^{1}H n.m.r. spectroscopy and gas chromatography were used to follow the kinetics of the TEOS transformation involving hydrolysis and condensation up to gelation or

Table 1
The effect of the type of the catalyst on the rate of transformation and gelation of TEOS and on the morphology

Catalyst	Transformation t (h)[a]	Gelation t_{gel} (h)[b]	Morphology
TSA	0.05 (3 min)	9[c]	clear gel
DBTDL	4.5	4	opaque gel
D2000	9	4.5	microgels
BDMA	30	5	precipitates
None	100[c]	24[c]	precipitates

$T = 20°C$, $C_{catalyst} = 2$ mol%/TEOS, TEOS: IP or EtOH = 45:55 (volume ratio), H_2O:TEOS = 3:1 (mole ratio)
[a] Half-time of the reaction of TEOS, at conversion $\alpha_{TEOS} = 0.5$
[b] Time to macroscopic gelation or microgel or precipitate formation
[c] $T = 80°C$

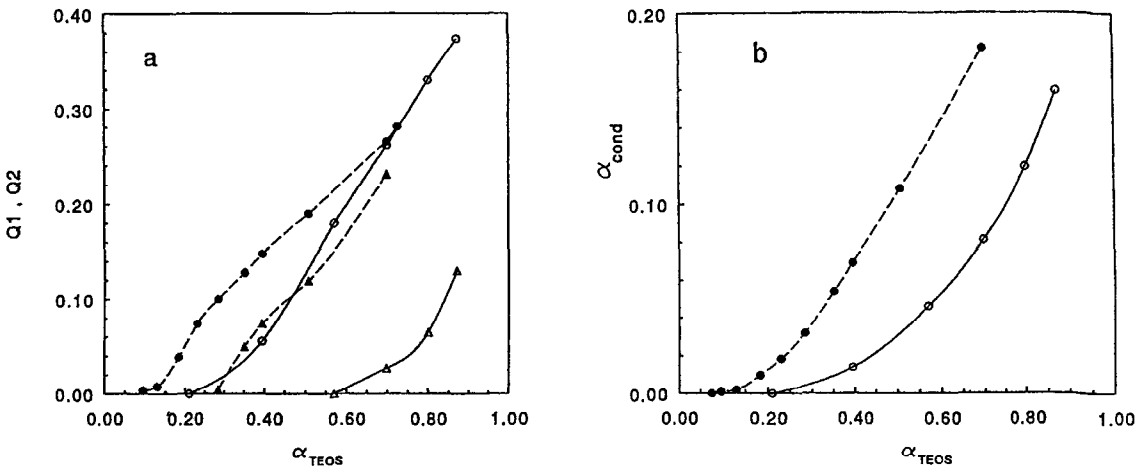

Fig. 2. Development of (a) fractions of the species Q_1 (○, ●) and Q_2 (△, ▲); and (b) condensation conversion α_{cond} determined by n.m.r. as a function of TEOS conversion, α_{TEOS}, in the polymerization of TEOS. — catalysis by TSA; - - -, catalysis by BDMA

phase separation. The rate of TEOS consumption, characterized by a half-time (reaction time at conversion $\alpha_{TEOS} = 0.5$) and given mainly by hydrolysis, decreases in the series of catalysts with increasing basicity TSA ≫ DBTDL > D2000 > BDMA ≫ no catalyst (see Table 1).

The catalysts govern the relative rates of hydrolysis and condensation and Fig. 1 shows the formation of the hydrolysed and condensed species determined by ^{29}Si n.m.r. during the sol–gel process catalysed by TSA and the nucleophilic BDMA. As is known [1] the acid catalysis promotes a fast hydrolysis resulting in the above-mentioned rapid TEOS conversion. A large fraction of highly hydrolysed products, i.e. speciesQ_0^3, Q_0^4, Q_1^2, Q_1^3 etc., is formed (cf. Fig. 1a, c) in contrast to the nucleophilic catalysis under which the extent of hydrolysis is lower and less hydrolysed products corresponding to the species Q_0^1, Q_1^1 prevail (see Fig. 1b, d). On the contrary, condensation is more effectively catalysed by the base catalyst and the condensed species, Q_1 and Q_2, are formed relatively earlier using BDMA compared with TSA (see Fig. 2a). The condensation conversion leading to Si-O-Si bonds defined as $\alpha_{cond} = \frac{1}{4}\sum_{i=1}^{4} iQ_i$ increases faster in this case (cf. Fig. 2b), typically of the base catalysis.

Slow condensation under acid catalysis by TSA was verified by GPC. Only oligomer products of molecular weight M_n ~1300 were found to be formed at room temperature during 24 h. This is also a result of significant cyclization [8,25] leading to the formation of small, internally cross-linked particles or cage-like structures [26,27]. Gelation is significantly delayed compared with the other catalysts used as shown in Table 1. Transparent gels appear in a reasonable time only on heating (see Table 1) and gelation sets in after a full conversion of TEOS. Using the nucleophilic catalysts BDMA and D2000, a more heterogeneous system is developed. High-molecular-weight products are formed from the very beginning because of fast condensation. The system phase separates and in the case of BDMA no gelation occurs. Precipitates or cloudy microgels emerge in the early stage at a low monomer conversion, α_{TEOS} ~0.15. The phase separation and gelation are manifested in ^{1}H n.m.r. by broadening of the signals corresponding to the CH_2 in EtOH, due to a lower mobility in the micro- or macrogel. The ^{29}Si n.m.r. signals of the condensed species involved in the particles or gel disappear after phase separation or gelation.

The morphology of the system prepared by using a higher concentration of D2000 becomes more homogeneous because of the solubilizing effect of poly(oxypropylene) chains on silica. Polymerization leads to an opalescent continuous gel without formation of microgels.

The formation of hybrid networks proceeds in the presence of both TSA and the nucleophilic D2000. The latter is employed as an epoxide hardener. The relative concentration of these catalysts was found to be crucial for the sol–gel reaction kinetics, SiO_2 network build-up and morphology of the silica phase, as shown in Table 2 and Fig. 3. In the case of diamine D2000, the concentration of catalytically active nucleophilic amine groups is considered. Since also the absolute content of D2000 affects the morphology as mentioned above, the polymerization of TEOS systems is investigated in the presence of a low and high content of D2000, i.e. about 2 (Table 2) and 21 mol% NH_2 relative to TEOS (Fig. 3), respectively. The latter models the composition in the hybrid system. It was found that an excess of the nucleophilic amine groups in D2000 compared with the TSA concentration results in a slow conversion of TEOS because of the slow hydrolysis and a fast appearance of microgel particles or a transparent continuous gel at a low or high content of D2000, respectively. In the region with an excess of TSA, an increase in the relative concentration of TSA dramatically accelerates hydrolysis and retards formation of the clear gel (see Table 1 and Fig. 3).

In agreement with literature data [11,28,29], the results indicate the two-step procedure to be an optimum method for fast inorganic structure formation. This process consists in our case of prehydrolysis of TEOS with acid TSA

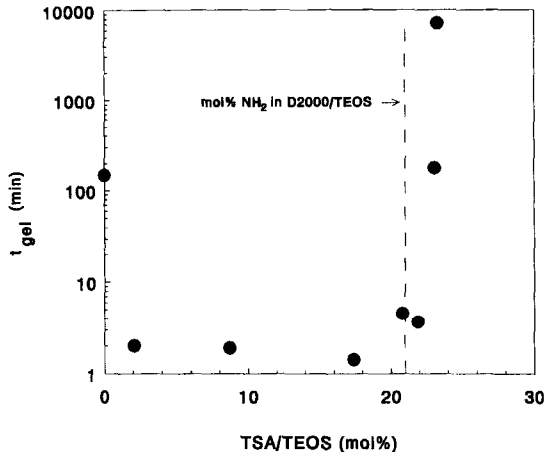

Fig. 3. Time of TEOS gelation, t_{gel}, in the presence of the catalysts TSA and D2000 as a function of concentration of TSA. $[NH_2]_{in\ D2000}$ = 21 mol%/TEOS; TEOS:IP = 45:55 (by volume), T = 23°C

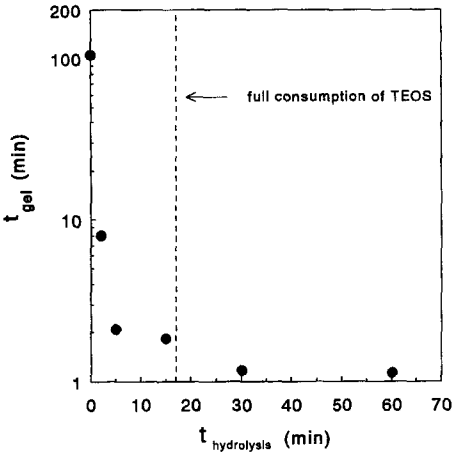

Fig. 4. Time of TEOS gelation catalysed by D2000 as a function of the time period of the acid prehydrolysis using 2 mol% TSA/TEOS. $[NH_2]_{in\ D2000}$ = 21 mol%/TEOS; TEOS:IP = 45:55 (by volume), T = 23°C

followed by formation of a network in the presence of nucleophilic D2000. Gelation at the D2000-catalysed polymerization of TEOS was significantly accelerated by acid prehydrolysis. The dependence of gelation time t_{gel} on the time of hydrolysis in the first step is shown in Fig. 4. All the monomer is hydrolysed within 17 min by using 2 mol% of TSA/TEOS (relative to TEOS). However, even 5 min of hydrolysis, corresponding to the TEOS conversion of more than 50%, is sufficient to initiate the subsequent condensation reaction in the basic medium in the second step, which is much faster than polymerization of the nonhydrolysed TEOS. Acid prehydrolysis of TEOS also prevents precipitation of silica or microgel formation. Clear gels are built up in the subsequent nucleophilic-catalysed polymerization even in the case of the small content of D2000. Based on these results of the model system, the TEOS prehydrolysis for 1 h in the presence of 2 mol% of TSA/TEOS was taken as the standard method for preparation of the hybrid networks.

3.2. Formation of the hybrid networks

Kinetics of the sol–gel transition in the system DGEBA–D2000–TEOS is not affected by the presence of the epoxide. Only a small retardation due to the dilution effect was observed. The influence of D2000, however, is substantial, as discussed above. Since preparation of the organic–inorganic hybrid was catalysed with TSA, the presence of base D2000 makes the formation and structure dependent on the relative concentration of both catalysts and on the method of preparation, as in the case of the model system.

Three synthetic procedures described in the Experimental were used to prepare hybrid 'simultaneous' and sequential IPNs differing in which network was formed first and in the catalysis. The epoxide system DGEBA–D2000 gels in 10 h at 80°C, while the sol–gel process is much faster under given conditions, even at room temperature (cf. Fig. 4). Hence, in a mixture of all components using the one- or two-stage process, the silica network is built up sooner, followed by gelation of the epoxide system. In the third sequential procedure, the epoxide network was prepared first and the silica structure grew within the organic rigid gel medium. All the hybrids prepared using IP as a diluent were optically clear. The reaction and catalytic conditions during the three procedures of hybrid synthesis were as follows.

3.2.1. One-stage process

Both the acid and polymeric amine D2000 catalysts are

Table 2
Rate of transformation and gelation of TEOS depending on relative concentrations of catalysts TSA and D2000

TSA mol%/TEOS	NH_2 in D2000 mol%/TEOS	Transformation at T = 20°C t^a	Gelation at T = 80°C t^b_{gel}	Morphology
2.3	—	3 min	10 h	clear gel
2.3	1.8	6 min	> 150 h	clear gel
2.3	2.3	72 h	60 min	microgels
2.3	3.1	> 150 h	30 min	microgels
—	2.3	15 h	10 min	microgels

TEOS:IP = 30:70 (by volume)
[a] Half-time of the reaction of TEOS at α_{TEOS} = 0.5
[b] Time to macroscopic gelation or microgel formation

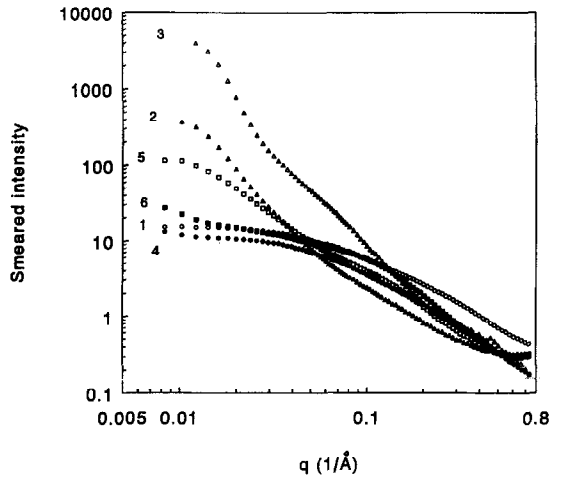

Fig. 5. SAXS profiles of TEOS polymerized using various catalysts and one-stage or two-stage procedures. Catalysis by 1, ○ TSA; 2, ▲ D2000 (20 mol% NH_2/TEOS); 3, △ BDMA; 4 ● DBTDL; 5, □ one-stage process (2 mol% TSA/TEOS, 20 mol% NH_2 in D2000/TEOS); 6, ■ two-stage procedure; 1st step 2 mol% TSA/TEOS, 1 h, 2nd step 20 mol% NH_2 in D2000/TEOS

present in the reaction mixture in the initial stage and their relative concentrations determine the reaction kinetics and structure of the silica phase. While the content of TSA is 2 mol%/TEOS, the concentration of the catalytically active NH_2 groups in D2000 diamine is 21 mol%. This implies that the amine is in high molar excess compared with TSA and the whole sol–gel process, i.e., both hydrolysis and condensation, is in fact catalysed by the nucleophile. Gelation of TEOS sets in after 81 min at room temperature and the epoxide network is formed later by increasing the temperature.

3.2.2. Two-stage process with prehydrolysis of TEOS

The procedure consists of prehydrolysis of TEOS in acid medium in the first stage followed by silica formation in the presence of both TSA and D2000 in the second stage and subsequent gelation of the epoxide system. The hydrolysis proceeds under acid catalysis and condensation is promoted by the amine which is in excess in the second step. Polymerization of TEOS is very fast in this case and gelation sets in within 1–2 min at room temperature (cf. Fig. 4).

3.2.3. Two-stage process with the preformed epoxide network

The preformed epoxide network is swollen in TEOS and the sol–gel process proceeds within the organic gel under the acid catalysis of TSA because the amine D2000 already incorporated in the network is ineffective as a catalyst. After swelling at room temperature, all Si-containing species could be extracted from the sample. This indicates: (a) quite a slow polymerization of TEOS and silica network build-up under these acid conditions; and (b) no binding of the inorganic components to the epoxide network occurring until this moment. After curing at 90°C the Si-containing components cannot be extracted from the network as a result of a strong interaction with the epoxide network or formation of a continuous interpenetrating epoxide–silica network.

3.3. Structure of the silica phase

SAXS measurements used to study the silica structure show that most of the intensity profiles reveal a linear part in the limited region of the double logarithmic plot of the intensity *versus* the scattering vector characteristic of fractals. The structures under study were described by the fractal dimensions, however, the linear regions are relatively short so that any discussion of the fractal behaviour must be taken with care. The gradual evolution of the structure is discussed in another paper [30]. In addition to the organic–inorganic hybrid a model TEOS system prepared under the same conditions was studied.

3.3.1. Model TEOS system

The scattering curves in Fig. 5 indicate that the structure formed in the presence of D2000 (curve 2) is similar to that prepared using a typical basic catalyst BDMA (curve 3). Both systems exhibit a high intensity at low angles corresponding to large heterogeneities and a rather steep slope of the curves, indicating compactness of the structures as observed in base-catalysed systems [1]. On the other hand, catalysis by pH neutral DBTDL (curve 4) leads to a more homogeneous structure similar to that produced under acid catalysis by TSA (curve 1). The intensity profiles of the optically transparent gels prepared by the acid and DBTDL catalysis are interpreted as open mass fractals of small heterogeneities with fractal dimension $(D_m)_{TSA} = 2.2$ and $(D_m)_{DBTDL} = 2.5$. The higher fractal dimension in the DBTDL-catalysed system may refer to the participation of reactions between monomer and large molecules (monomer–cluster growth model) compared with the cluster–cluster reaction in the acid medium [1]. This difference is a result of a relatively slower hydrolysis and monomer consumption with respect to condensation in the case of DBTDL catalysis (see Table 1). The monomer is available for condensation even at a late stage, in contrast to the acid catalysis where it is consumed very quickly and condensation proceeds during participation of clusters only. Fig. 5 also shows the SAXS profiles of the TEOS system containing both TSA and D2000 modelling the catalytic conditions in the hybrid. Scattering curve 6 of the silica gel prepared by the two-stage procedure involving acid prehydrolysis of TEOS reveals small heterogeneity domains and resembles that formed under acid catalysis by TSA. On the contrary, the one-step polymerization of TEOS results in a structure (curve 5) more similar to that observed using D2000 as a catalyst. Further curing at an increased temperature and drying to prepare xerogels leads to the structure densification and compact surface fractals are formed in the case of acid catalysis.

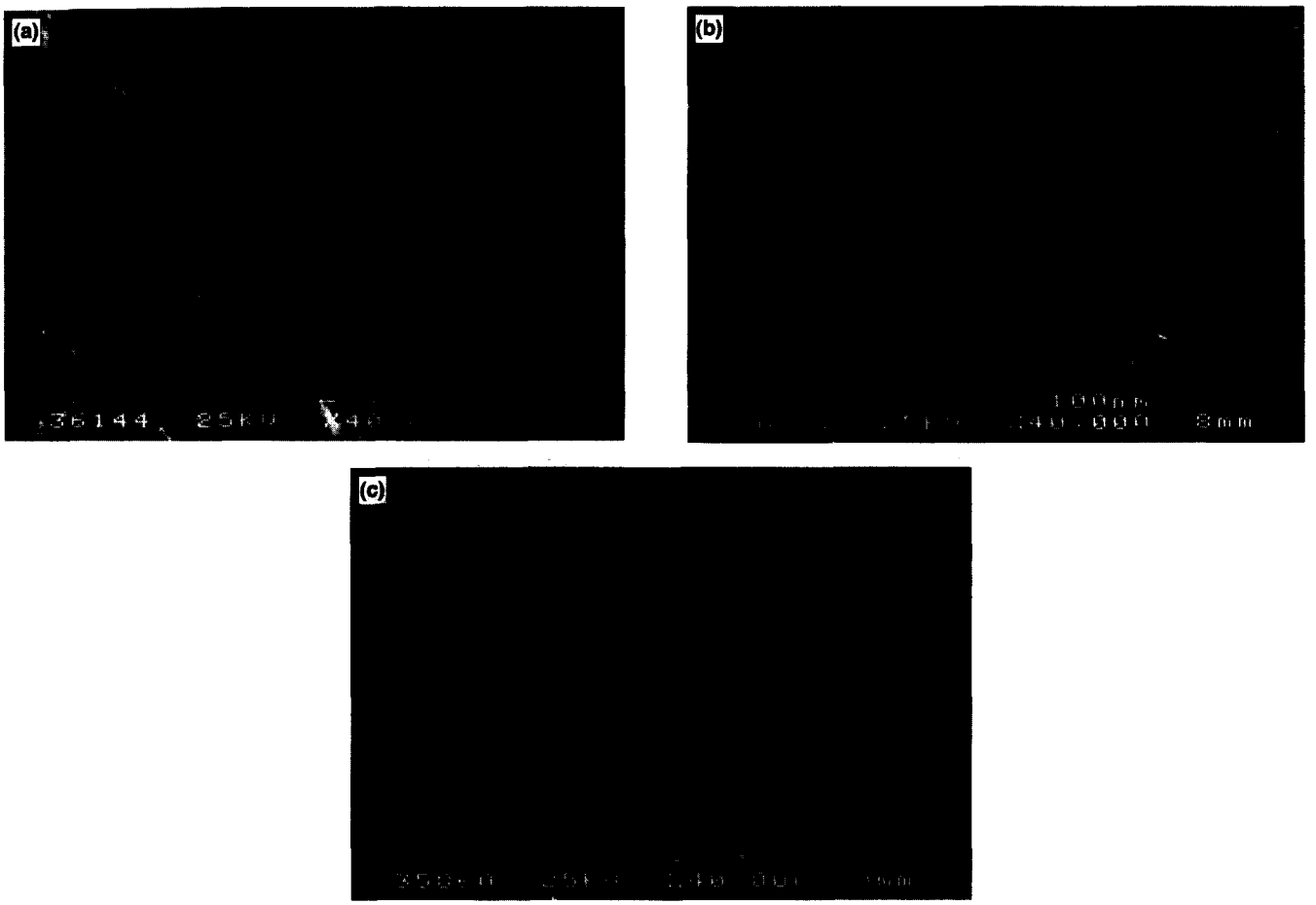

Fig. 6. Micrographs of the hybrid IPNs DGEBA–D2000–TEOS prepared by: (a) one-stage process; (b) two-stage process with acid prehydrolysed TEOS; (c) two-stage process with preformed epoxide network

3.4. Hybrid network DGEBA–D2000–TEOS

Heterogeneous, microphase-separated hybrid IPNs are optically transparent because of the small size of the silica domains. The morphology and size of the domains were determined by electron microscopy and their inner structure was followed using SAXS. SEM pictures and SAXS profiles of the hybrids, prepared by the three different procedures and subsequently dried, are given in Figs 6 and 7.

3.4.1. One-stage process

The SEM graph of the hybrid system in Fig. 6a shows small dispersed particles of 20–70 nm in diameter which are aggregated in large irregular aggregates of size ~100–300 nm. SAXS profiles of the three types of hybrids in Fig. 7 exhibit in the one-stage case (curve 1) the highest intensity at low angles and the steepest intensity curve, corresponding to the largest and most compact structure heterogeneities in agreement with the model system. This is a result of the base catalysis during the one-stage polymerization, as shown above. The fractal dimension of the silica domains gradually increases during the reaction [30] up to $D_m = 2.3$ at the gel point and $D_m = 2.5$ at $t = 3t_{gel}$. Participation of the monomer–cluster aggregation [1] may describe formation of such a relatively compact structure. Drying of the gel at high temperature leads to further structure densification; $(D_m)_{dry} = 2.7$.

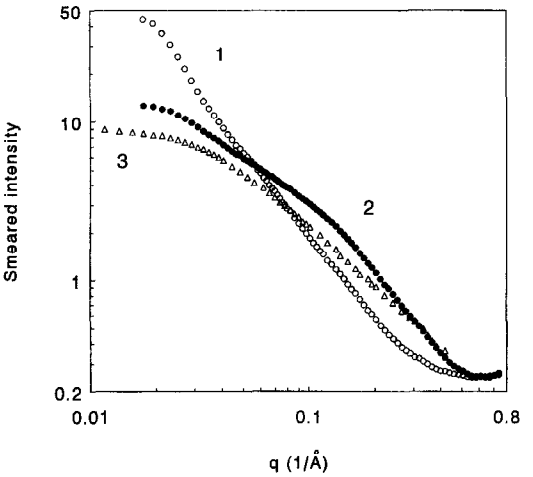

Fig. 7. SAXS curves of the dry hybrid DGEBA–D2000–TEOS prepared by: 1, one-stage process; 2, two-stage process with acid prehydrolysed TEOS; 3, two-stage process with preformed epoxide network

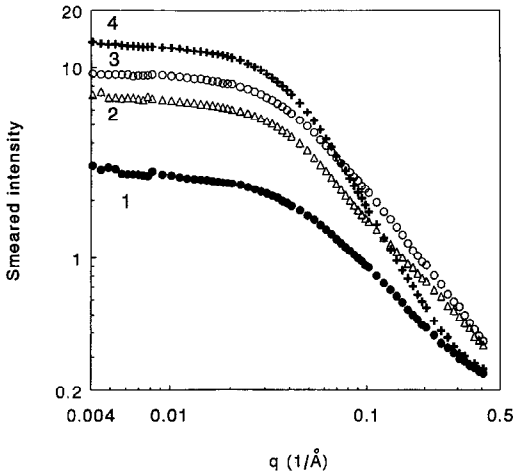

Fig. 8. SAXS curves of the hybrids DGEBA–D2000–TEOS prepared by the two-stage procedure with preformed epoxide network catalysed by TSA or DBTDL. 1: ● TSA, 3.1 wt% SiO_2 (TEOS:IP = 5:95); 2: △ TSA, 7.8 wt% SiO_2 (TEOS:IP = 20:80); 3: ○ TSA, 11.4 wt% SiO_2 (TEOS:IP = 40:60); 4: + DBTDL (TEOS:IP = 40:60)

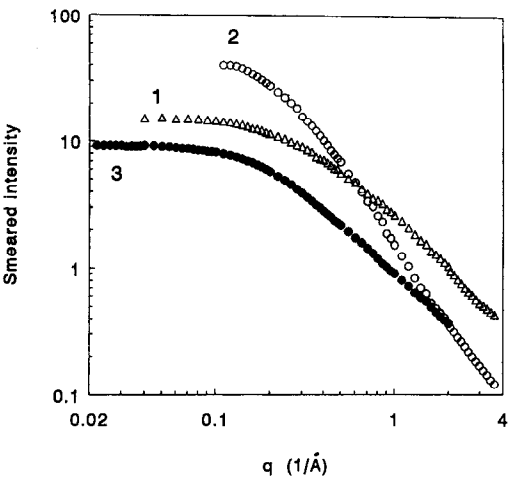

Fig. 9. SAXS curves of the polymerized TEOS and the hybrid DGEBA–D2000– TEOS. 1: △ polymerized TEOS (2 mol% TSA/TEOS) at the gel point; 2: ○ polymerized TEOS (2 mol% TSA/TEOS) after drying; 3: ● TEOS polymerized in the DGEBA–D2000 network (2 mol% TSA/TEOS) after drying—hybrid prepared by the two-stage procedure with the preformed epoxide network

3.4.2. Two-stage procedure with the acid prehydrolysis of TEOS

The structures are smaller compared with the one-stage case and the heterogeneities of 50–100 nm in the micrograph in Fig. 6b seem to be continuously interconnected within the organic medium. SAXS profiles reveal that loose polysiloxane aggregates with the low fractal dimension, $D_m = 1.7$ [30] are formed at room temperature. The low value of the fractal dimension is typical for a diffusion-limited cluster–cluster [30] reaction. In the two-stage procedure, the majority of monomeric species is consumed during the acid-catalysed prehydrolysis step. Therefore, the monomer–cluster reactions are unimportant in the subsequent polycondensation catalysed by the nucleophile and open ramified structures appear by preferred cluster–cluster reactions similar to the acid-catalysed system. The intensity curve of the scattered radiation develops during the polymerization and two linear parts in the double logarithmic plot appear in later reaction stages and at drying (see Fig. 7, curve 2) revealing two length scales of the structure. Such an intensity curve may be interpreted as a large aggregate composed of smaller, more compact particles. Drying results in densification mainly of the 'particles', while the aggregates remain less compact; $(D_m)_{particle,dry} = 2.7$ and $(D_m)_{aggregate,dry} = 2.0$. Inefficiency in postcuring to densify the aggregates may be explained by steric restrictions in the network. The sol–gel process is much faster than gelation of the epoxide system; however, during the hybrid drying at high temperature, the epoxide network is completely built-up. As a result, the silica aggregation by interparticle reaction leading to densification of aggregates at drying is sterically restricted by the epoxide network. On the contrary, an intraparticle condensation reaction is not inhibited.

3.4.3. Two-stage procedure with the preformed epoxide network

SEM micrographs show that the smallest inorganic domains of size ~10–20 nm are formed by sequential polymerization with the preformed epoxide network (cf. Fig. 6c). The structure is very fine and no larger agglomerates appear. The intensity of SAXS profiles at low angles in Fig. 8 grows with increasing content of SiO_2 in the hybrid as the amount of silica domains is enhanced. However, the size of siloxane fractal structures formed within the epoxide network does not grow with the silica content; $d\,(=2\pi/q_{min}) \sim 150$ Å (see Fig. 8), which is in agreement with the results of SEM. The silica structure formed under acid catalysis in this case is the most open and weakly ramified compared with the one- and two-stage 'simultaneous' systems discussed above, as indicates a small slope of the corresponding curve 3 in Fig. 7. Low fractal dimension $D_m = 2.0$ was determined even in the dry hybrid. The compactness of the system catalysed with TSA remains almost independent of the silica content (cf. curves 1–3 in Fig. 8) and fractal dimension ranges as $D_m =$ 1.9–2.2. Obviously, the acid catalysis with TSA promoting a more homogeneous inorganic structure was operative during the whole sol–gel process. In addition to the catalytic conditions during the reaction, the steric restrictions to the growth of the siloxane cross-linked structures due to the rigid organic matrix are important. The silica build-up proceeds in this case within the epoxide network, preventing formation of large inorganic domains. The influence of the reaction medium rigidity of the epoxide network imposed on the sol–gel process in the hybrid is shown in Fig. 9 by comparing with the model TEOS system. One can see the significant increase in compactness—fractal dimension—manifested by the slopes of the scattering curves, by drying

of the polymerized TEOS from the state close to the gel point (curve 1) up to the state of the xerogel (curve 2). In contrast, TEOS polymerized in the epoxide network exhibits an open silica gel structure in the dry hybrid DGEBA–D2000–TEOS (curve 3) similar to the non-dried model. Obviously, restrictions to an aggregation and structure densification by the preformed epoxide network are operative in the hybrid IPN. The effect of the cross-linking density on the silica particle size was also determined by Wen and Mark [31]. The neutral catalysis by DBTDL (curve 4 in Fig. 8) leads to a more compact structure, $D_m = 2.7$, in agreement with the data obtained for the model system as a result of a possible combined monomer–cluster and cluster–cluster aggregation. The size of silica domains, however, is limited by the epoxide network in the same way as in the case of the acid catalysis (cf. Fig. 8).

The Wilkes morphological model [2] of an organic–inorganic hybrid was based on SAXS data of the hybrids prepared by cross-linking of alkoxysilane endcapped polymers. The intensity curves showed an interference maximum revealing a regular space arrangement with silica domains formed at the end of polymeric alkoxy precursors. However, no maximum was observed in our IPNs because of irregular space arrangement of the silica structure in the DGEBA–D2000–TEOS hybrid. Generally, the structure and morphology of sol–gel polymerized systems are determined by several factors that are crucial to the structure of the DGEBA–D2000–TEOS hybrid.

1. The reaction mechanism such as relative rates of hydrolysis and condensation is of great importance [1,8]. The effect of catalysts, including polymeric catalyst D2000, on the reaction mechanism and structure was discussed above. Landry et al. [7] observed that the kinetics of TEOS polymerization is not significantly affected in the presence of the organic polymer PMMA, contrary to our catalytically active polymer system. In spite of that, silica structure in hybrids resembles our results. Open structures with $D_m \sim 2$ of size $d < 10$ nm and small silica particles 2–4 nm were determined under acid catalysis and 100–200 nm large compact aggregates with $D_m \sim 2.8$, including 1–5 μm large clusters, were observed using base catalysis.
2. The effect of steric conditions on silica structure in a hybrid was not often discussed in the literature [19,31]. The idea of restriction of aggregate growth by the rigid network matrix was supported by the results of Wen and Mark [31], however, Bauer et al. [19] did not find any dependence of the silica domain size on the cross-linking density.
3. The microphase separation plays an important role and relative rates of polymerization, phase separation or vitrification influence the morphology. In the case of fast polymerization and early gelation the microphase separation is arrested and smaller heterogeneities appear. Consequently, much faster gelation after acid prehydrolysis of TEOS compared with the one-stage process may also be a reason of a finer morphology in the 'two-stage' hybrid.
4. In organic–inorganic hybrids, an interphase interaction by chemical grafting [19,32] or physical interaction [7] of the silica domains with a polymer make the system more miscible and a finer morphology results. The siloxane structures are more hydrolysed under acid catalysis, leading to stronger interaction of SiOH groups with C-OH of the epoxide network and to more homogeneous morphology, as observed in the DGEBA-2000–TEOS hybrid with the preformed epoxide network.

Physical interaction in the system PMMA–TEOS due to H-bonding between silanols and C=O groups of the polymer was proved to lead to better mixing and delay of phase separation [7]. The important effect of grafting between the epoxy and silica networks on the final hybrid morphology was found by Bauer *et al.* [19]. His interpretation of SAXS data showed differences in phase mixing in simultaneous and sequential IPNs. The sequential IPN with preformed epoxide network was strongly phase separated with slopes of the SAXS profile in the Porod region equal to $x = 4$ (cf. paragraph on SAXS) compared with our result, $x = 2$. On the contrary, grafting during simultaneous polymerization promoted considerable phase mixing in IPN with the slopes in the SAXS linear region, $x = 2$ [19]. The different structure results of some of ours and Bauer's hybrid system with the same composition DGEBA–D2000–TEOS may be attributed to the slightly different synthesis procedure. The reaction conditions during the sequential polymerization, in the case of Bauer's IPN were milder as the sol–gel process proceeded at a low temperature only. Under these conditions the grafting is less probable and stronger phase separation is to be expected. In our case the hybrids were cured at high temperature and the grafting takes place in simultaneous, as well as sequential, IPNs. The interphase interaction due mainly to grafting was proved by dynamic mechanical analysis and will be presented in the next paper. The size of the silica domains observed by Bauer agrees with our data in the case of the sequential systems, ~10 nm, however, no larger aggregates were detected by Bauer in the simultaneous IPNs contrary to our observation in the 'one-step' hybrids. In fact, during our one-stage process the silica phase was formed faster while it was epoxide network under Bauer's condition of 'simultaneous' polymerization owing to the later addition of water. Hence, growth of larger siloxane aggregates was sterically restricted in the latter case.

4. Conclusions

The results show that the presence of organic epoxide–amine components and the method of preparation control the evolution of the silica structure in the organic–inorganic

hybrid IPN, DGEBA–D2000–TEOS. The sol–gel process is acid-catalysed with TSA; however, the epoxide hardener D2000 of the epoxide–amine system affects the polymerization of TEOS and morphology because it serves as a polymer nucleophilic catalyst. The D2000 is not effective in catalysis of TEOS hydrolysis but it appreciably accelerates gelation. In addition, the poly(oxypropylene) chain of D2000 ensures a good solubilization of the silica and as a result, transparent gels are formed during TEOS polymerization, in contrast to the usual base catalysis, e.g. by BDMA.

The one- and two-stage procedures used for the hybrid preparation differ in the relative ratio of the catalyst concentrations of TSA and D2000 during the hydrolysis and polycondensation, which is crucial for the structure development. Therefore, the rate of the hybrid network formation and structure can be controlled by the method of preparation. The structure is determined by the early stage of the sol–gel process, i.e. by the hydrolysis step and the corresponding catalytic conditions. Compact and large silica structures were observed under the nucleophilic catalysis in the 'one-stage' hybrid, whereas open polymeric structures of smaller aggregates composed of fractal 'particles' were formed during the two-stage procedure with the acid prehydrolysed TEOS. Moreover, this two-stage process resulted in a much faster gelation of the silica.

In these 'simultaneous' IPNs, the silica network is formed faster than the epoxide one and its structure is not influenced by the presence of the epoxide. However, in the case of the sequential two-stage procedure, the preformed epoxide network suppresses growth of the silica aggregates by interparticle condensation and the relatively smallest silica domains are formed.

In forthcoming papers the evolution of the inorganic phase structure within the hybrid [30] determined by SAXS and the mechanical properties of the IPNs revealing the reinforcement of the rubbery network are described.

Acknowledgements

The authors wish to thank the Grant Agency of the Czech Republic for support of the work (projects Nos 203/94/0819 and 203/96/1387) and the US-Czech Science and Technology Program (grant No. 920-34).

References

[1] Brinker CJ, Scherer GW. Sol-Gel Science. Academic Press, New York, 1989.
[2] Wilkes GL, Orler B, Huang HH. Polym Prepr 1985;26:300.
[3] Noell JLW, Wilkes GL, Mohanty DK, McGrath JE. J Appl Polym Sci 1990;40:1177.
[4] Schmidt H. Mater Res Soc Symp Proc 1990;3:171.
[5] Mark JE, Pan SJ. Makromol Chem 1982;3:681.
[6] Surivet F, Lam TM, Pascault JP, Mai C. Macromolecules 1992;25:5742.
[7] Landry CHJT, Coltrain BK, Brady BK. Polymer 1992;33:1486.
[8] Iler RK. The Chemistry of Silica. Wiley Interscience, New York, 1979.
[9] Novak MB. Advanced Materials 1993;5:422.
[10] Assink RA, Kay BDJ. Non-Crystalline Solids 1988;99:359.
[11] Schaefer DW, Keefer KD. Phys Rev Lett 1984;53:1383.
[12] Schaefer DW. Science 1989;243:1023.
[13] Krug H, Schmidt H. First European Workshop on Hybrid Organic-Inorganic Materials. Chateau de Bierville, France, 1993, p. 127.
[14] Snijkers-Hendrickx IJM, Oomen MVJL. First European Workshop on Hybrid Organic-Inorganic Materials. Chateau de Bierville, France, 1993, p. 237.
[15] Kasemann R, Schmidt H. First European Workshop on Hybrid Organic-Inorganic Materials. Chateau de Bierville, France, 1993, p. 171.
[16] Schubert U. First European Workshop on Hybrid Organic-Inorganic Materials. Chateau de Bierville, France, 1993, p. 113.
[17] Novak BM, Auerbach D, Verrier DC. Chem Mater 1994;6:282.
[18] Dave BC, Dunn B, Valentine JS, Zink J. Anal Chem 1994;66:1120.
[19] Bauer JB, Liu D-W, Jackson CL, Barnes JD. Polym Adv Technol 1995;7:1996.
[20] Kelts LW, Armstrong NJ. J Mater Res 1989;4:423.
[21] Marsmann H. NMR Basic Principles and Progress. Springer, Berlin, 1981, p. 65.
[22] Kratky O, Pilz I, Schmitz PJ. J Colloid Interface Sci 1966;21:24.
[23] Glatter O, Gruber K. J Appl Crystallogr 1993;26:512.
[24] Schmidt PW. The Fractal Approach to Heterogeneous Chemistry. Avnir D, editor. John Wiley, New York, 1989.
[25] Kelts LW, Armstrong NJ. Better Ceramics through Chemistry III. Brinker C, Clark DE, Ulrich DR, editors. Mat Res Soc, Pittsburg, 1988, p. 519.
[26] Himmel B, Gerber T, Burger H. J Non-Crystalline Solids 1990;119:1.
[27] Ng LV, Thompson P, Sanchez J, Macosko CW, McCormick AV. Macromolecules 1995;28:6471.
[28] Fleming JW, Fleming SA, Kelly D. Ultrastructure Processing of Advanced Materials. Uhlmann DR, Ulrich DR, editors. John Wiley, New York, 1992, p. 77.
[29] Brinker CJ, Scherer CW. J Non-Crystalline Solids 1985;70:301.
[30] Matějka L, Pleštil J, Dušek K. Non-Crystalline Solids, in press.
[31] Wen J, Mark JE. Rub Chem Tech 1994;67:807.
[32] Girard-Reydet E, Lam TM, Pascault JP. Macromol Chem Phys 1994;195:149.